JOURNAL OF MATERIALS SCIENCE 22 (1987) 1724–1732

The falling weight impact test applied to some glass-fibre reinforced nylons

Part 2 *Some results and interpretations*

A. E. JOHNSON
Pilkington Brothers plc, Research and Development Laboratories, Lathom, Ormskirk, Lancashire L40 5UF, UK

D. R. MOORE, R. S. PREDIGER
ICI Petrochemicals and Plastics Division, Wilton, PO Box 90, Middlesbrough, Cleveland TS6 8JE, UK

P. E. REED, S. TURNER
Department of Materials, Queen Mary College, Mile End Road, London E1 4NS, UK

Measurements on five glass-fibre reinforced compounds have shown that at fibre weight fractions of 0.3 and 0.5 increased mean fibre length confers greater resistance to impact as measured by a conventional flexed-plate method. The results were consistent with notional fracture surface energies that were deduced from the lengths of crack generated by various low-energy blows and from the lengths recorded by flash photography at various stages of impact events. The velocity of impact was not influential over the range investigated (1 to 5 m sec^{-1}). The investigation was not straightforward because when a test specimen of this class of material is impacted at room temperature the observed response is either heavily contaminated with extraneous vibrations due to the absence of an electrical filter or of questionable purity due to the presence of a filter. In that respect, and others, the paper is linked to an earlier one (*J. Mater. Sci.* **21** (1986) 3153).

1. Introduction

This paper presents impact test data obtained on five glass-fibre reinforced nylon compounds by a flexed plate method in three laboratories. Ordinarily, such an introductory statement would probably be followed by a report in which the issue of interlaboratory variability featured quite strongly, but that is not so in this case, at least partly because the paper to which this one is a sequel [1] ended with the words ". . . it follows, also, that simple inter-laboratory comparisons of the type likely in "round-robin" exercises will generally yield results implying poor agreement".

That earlier paper was a necessary prelude to this one simply because the primary data that emerge from an impact test on a specimen made from a material such as a glass-fibre reinforced nylon are not easy to interpret and the secondary data, i.e. the impact strengths and impact energies that are derived from the primary data by integration etc., do not necessarily convey true statements about the impact resistance. For example, an unfiltered force–time signal is the impact response curve of the specimen overlain by extraneous vibrations and, in the case of the reinforced nylons, one could even say that the response curve is obscured by the noise; on the other hand, an electrically filtered force–time curve is generally free of the extraneous vibrations but, by the same token, is also bereft of the fine structure of the true response. Thus, when three laboratories have different filtering procedures because they exist for different purposes the data that they generate on a common sample and the interpretations that they place on their results will inevitably differ. That issue and others of a related nature were discussed in the earlier paper and largely disposed of as far as this particular experimental programme is concerned. The satisfactory rationalization of the data owed much to the use of flash photography of the specimen at a precisely timed moment during the impact event. That technique enabled the development of damage in the specimen to be associated with particular features on the response curve. Those critical features were not always overtly dominant. The photography, coupled with certain other independent experiments, led to two very important conclusions for these particular specimens and samples (and doubtless also for many others), namely:

(i) the failure process can start early in the impact event and long before the force reaches a maximum, and

(ii) the fracture process *per se* has reached completion before the recorded force has reduced to zero and more energy is absorbed thereafter by extraneous processes not directly associated with impact failure.

Thus forearmed, and with the reader forewarned, we now pass on to some consideration of the impact resistance of five glass-reinforced nylon compounds.

0022–2461/87 $03.00 + .12

TABLE I Sample codes and material specifications

Code	Description
PA-1	Nylon 66 + nominally 0.5 weight fraction of short glass fibres
PA-2	Nylon 66 + nominally 0.5 weight fraction of longer glass fibres than PA-1
PA-3	As PA-2 but approximately 0.3 weight fraction
PA-4	Nylon 66 + nominally 0.3 weight fraction of short glass fibres + pigment
PA-5	Nylon 6 + nominally 0.3 weight fraction of short glass fibres

2. Experimental details

The five compounds studied in this investigation were described in the previous paper [1] but the essential facts are reproduced here again for convenience, see Table I and below.

The compounds were injection-moulded on a Demag D80 machine using the following conditions:

1st stage injection	= 20 bar (2 MPa)
2nd stage injection	= 56 bar (5.6 MPa)
Back pressure	= 10 bar (1 MPa)
Melt temperature	= 280° C
Mould temperature	= 90° C
Screw speed	= 120 r.p.m.
Injection time	= 2.5 sec
Follow-up time	= 8 sec
Cooling time	= 30 sec

The major proportion of each sample was moulded into edge-gated discs 60 mm in diameter and about 2 mm thick. The mould had two nominally identical cavities but the mouldings have been distinguished by the letters L (left-hand) and R (right-hand). Thus specimens are identified where necessary by a code number such as PA-IL/33 which gives the sample (PA-1), the cavity (L) and the shot number (33). Subsidiary batches of mouldings were edge-gated discs, 100 mm in diameter and 3 mm thick.

Each collaborating laboratory, designated P, Q and W in this paper, had its own falling weight impact machine; that in Laboratory Q was a Ceast Advanced Fractoscope System Mark 3 and those in the other two laboratories were home-made. A description of the one in Laboratory W has been published [2]. In the tests, the specimens were freely supported on an annulus of radius 20 mm. The impactor had a hemispherical tip of radius 10 mm and the incident energy was far in excess of that needed to break the specimens. Tests were conducted at room temperature, at impact velocities of 1, 3 and 5 m sec^{-1}. All specimens were stored "dry".

In addition to the standardized impact tests, three subsidiary techniques were employed. These were photography of the specimen at various pre-selected instants during the impact event, which was referred to in Section 1; low-energy impact tests in which the specimen was damaged but not destroyed; glass-fibre length analysis of the moulded specimens [3].

The precisely timed photography was accomplished by use of a twin channel transient recorder (Nicolet 3091) which captured the force values on the first channel in the usual manner, and simultaneously determined the time when the photograph was taken by means of a large-area photodiode connected to the second channel. This enabled the start, intensity, and duration of the flash to be measured during each impact event. An electronic timing device was used to delay the flash by a pre-set interval. The delay circuit was connected to the first channel of the transient recorder so that the voltage rise from the force transducer triggered the pre-set delay. With this arrangement the time when the flash reached the maximum intensity could be determined with an accuracy equal to the time interval between successive points, which was 2 μsec for the fastest sweep-time. By progressively increasing the pre-set time delay for successive impact tests (each on a new specimen) a series of photographs was obtained covering all stages of the fracture process and enabling crack length to be correlated with energy absorbed. Other details of this technique are given elsewhere [4].

The low-energy impact tests entailed an incident energy lower than that needed to break or rupture the specimen but enough to inflict some damage or incipient damage that would otherwise be obscured if the incident energy had been excessive. These glass-fibre-reinforced nylons are particularly amenable to this approach because the fibres bridge the growing crack to some degree and thereby frustrate any tendency for the crack to propagate out of control, and by careful choice of incident energies successive stages of damage can be developed. For all five grades, the damage almost invariably took the form of a three-branched crack initiating at the point of impact. The three main branches grew radially, with occasional and temporary deviations from the main and expected directions [5]. The crack lengths could always be measured approximately by means of a ruler.

The apparatus used for the low-energy impacts (Laboratory Q) was not ideal for the task in that the requisite low incident energies could not be attained merely by reduction of the mass of the impactor and therefore the impact velocity was changed instead. With many materials it is essential that energy and velocity are independently varied but in view of the nature of these particular materials, and direct experimental evidence, it was deemed that the changes in impact velocity could be disregarded. Subsequent experiments have shown that judgement to be faulty in that the velocity and the energy exert separable influences on the degree of damage, but the main conclusions concerning the distinctions between the impact resistances of the five materials are not thereby invalidated and hence those recent results, which have arisen in the pursuance of a separate programme, will be reported later, in their rightful context and not here where they would encumber the argument rather than enlighten it.

Of the materials listed in Table I, three are standard, commercially available compounds and two (PA-2 and PA-3) are experimental grades that differ from the others mainly in having longer fibres than had been used in commercial moulding compounds. The differences embodied by the loose terms "short" and "long" glass fibres can be gauged from Fig. 1 which

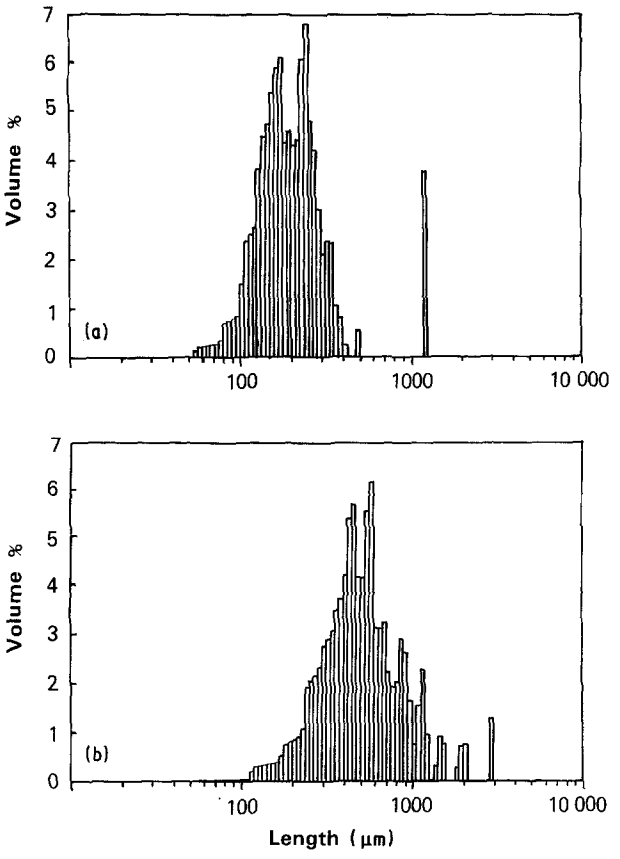

Figure 1 Distribution of fibre lengths. (a) PA-1 (weight-average length 238 μm, number-average length 178 μm; (b) PA-2 (weight-average length 601 μm, number-average length 432 μm).

shows the distributions of fibre lengths for compounds PA-1 and PA-2.

The experimental programmes carried out in the three laboratories were such as to provide some basis for interlaboratory comparisons but to avoid too much duplication, so that the effect of the critical variables could be explored as economically as possible. They also reflected the special interests of the collaborators. The primary measurement in all three machines was via a force transducer but there were differences in the way the signal was processed thereafter, the most important one being that Laboratories P and W used analogue cut-off filters (at 3.3 and 2.2 kHz, respectively) whereas Laboratory Q had optional use of a variable narrow-band filter (which was seldom used). The various disparities between the filtered and the unfiltered data for the 2 mm thick small edge-gated discs and the ambiguities in the interpretations were discussed in Part 1 [1] and hence they need not be reconsidered here, but in the interests of clarity cetain features of the force–time curves need to be identified and designated. Thus with reference to Fig. 2a and in reiteration of what was defined in the first paper, the first of the many peaks on the unfiltered force–time curves for the 2 mm thick mouldings of these nylon compounds has no physical significance in relation to the response of the specimen, whereas the second peak is thought to have significance; the latter feature has been designated Feature A. Accordingly, the tabulated data emanating from Laboratory Q relate to Feature A, to the peak associated with the maximum force and to the point at which the force has later reduced to zero (even though the physical significance of the last one is questionable). The filtered data for the 2 mm thick mouldings, shown schematically in Fig. 2b, have a peak near the origin* which probably corresponds to the first one in the unfiltered data and which is ignored as an artefact in this paper; thereafter, the extraneous vibrations are largely suppressed, there is usually a change of slope that could correspond to the Feature A referred to above and there are subsequently several peaks the first one of which is taken as a datum. The "first peak" is sometimes but not always the maximum force that develops during the impact event.

There is no extraneous small peak on the filtered force–time curves for the 3 mm thick mouldings. That lends credence to the supposition that the peak has no physical significance since the thicker specimen will have a different resonant frequency and different dissipative character from the thinner one so that the impulse transmitted to the total mechanical system, and hence its extraneous response, will be different. However, mouldings of materials such as these consist essentially of a set of differently anisotropic lamellae and one should never then invoke thickness as a simple concept; thus, it would be premature and imprudent for this argument to be pursued at this juncture.

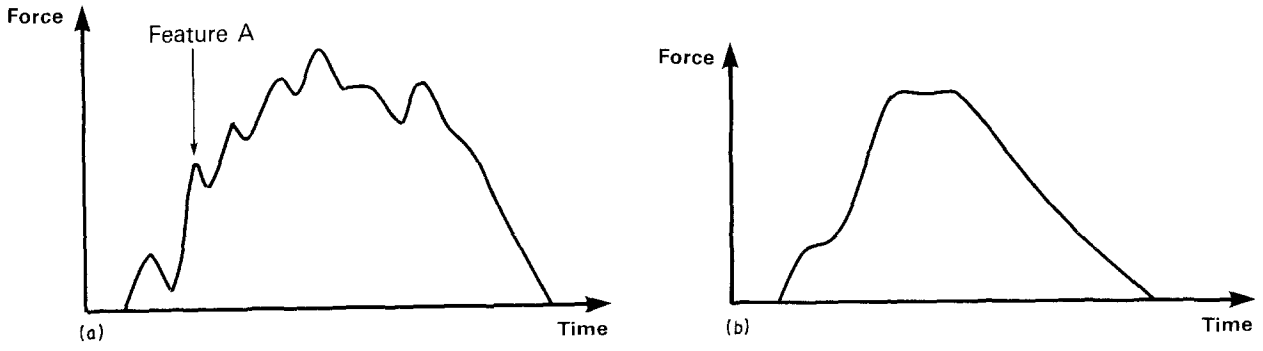

Figure 2 Schematic force–time responses. (a) Unfiltered signal, (b) filtered signal (cut-off beyond 2.2 kHz).

*A small peak is frequently observed in flexed plate impact testing and is often referred to in the literature as an "inertia peak", which is possibly slightly misleading in the associations it brings to mind.

TABLE II Comparison of impact resistance of specimens from left-hand and right-hand cavities (Laboratory Q)

Sample code	Impact velocity ($m\,sec^{-1}$)	Thickness ratio	Property ratio (right-hand cavity specimen/ left hand cavity specimen)				
			Peak force (Feature A)	Energy to peak (Feature A)	Max. force	Energy to max. peak	Total failure energy
PA-1	1	1.04	1.04	1.03	1.05	0.93	1.10
PA-1	5	1.04	1.15	0.83	0.92	1.13	0.94
PA-1 (filtered data)	5	1.04	1.20	0.92	1.06	1.33	1.08
PA-2	1	1.04	1.02	0.95	1.00	1.71	1.16
PA-3	5	1.02	1.14	1.05	1.12	1.31	1.15
Mean values (standard deviation)		1.04 (0.01)	1.11 (0.08)	0.96 (0.09)	1.03 (0.08)	1.28 (0.29)	1.09 (0.09)

3. Results

3.1. Property differences for specimens from right-hand and left-hand cavities

As a prelude to the presentation of the main body of the data, which is naturally directed towards a comparison of the impact resistances of mouldings made from the various grades, it is necessary for the performance of specimens from the left-hand cavity and the right-hand one to be compared. That necessity arises firstly because imbalances between the flow impedences associated with nominally identical cavities are a well known cause of variability in properties, and secondly because there was an obvious difference in the thicknesses of the members of the paired sets produced for these investigations.

The tests were carried out in Laboratory Q, on three of the grades, at two impact velocities and with a 9 kHz filter in one case. The numerical values of the extracted quantities, e.g. the force at Feature A, are not quoted directly but as ratios of the property value for right-hand cavity specimens to that for the left-hand cavity specimens (see Table II), partly because the use of such ratios simplified the task of effecting a comparison and party so as not to introduce specific values of the quantities into the paper prematurely. If there is no effect attributable to specimen thickness, the ratios should be equal to unity or should be randomly distributed about that value. The mean values of the ratios suggest that there is such an effect and, though small, it could distort comparisons between sets of data if appropriate steps were not taken to eliminate cavity bias; that was done thereafter either by restricting the source of specimens for particular comparisons or by random choice of specimens for the sets.

There may be more to the differences than is apparent from the tabulated ratios because the low-energy-blow experiments showed a lower resistance to cracking in specimens from the left-hand cavity. This can be seen, for example, in Fig. 3 where total crack length is plotted against incident energy for specimens moulded from PA-1, but it was also manifest as a subtle difference in the appearance of left-hand and right-hand specimens after blows of such low energy that no specific cracks could be identified under a hand lens.

This topic will be avoided, rather than pursued, in the rest of this paper.

3.2. The effect of impact velocity

When impact tests are directed towards the location of the ductile–brittle transition the impact velocity can be varied somewhat analogously to the temperature, since both of those variables will serve to identify the region beyond which the molecular relaxation processes cannot respond adequately to the excitation function. Such considerations are largely irrelevant to these particular experiments since at impact testing rates at room temperature the materials are not ductile in any viscoelastic sense. Instead, impact velocity was varied because of the effect that such variation would have on the shock wave generated by the impact and on the associated response of the specimen.

All five grades were impacted at 3 and 5 $m\,sec^{-1}$ in Laboratory P. There seems to be no clear trend with velocity, though for individual grades the evidence could be interpreted otherwise. The data are given in

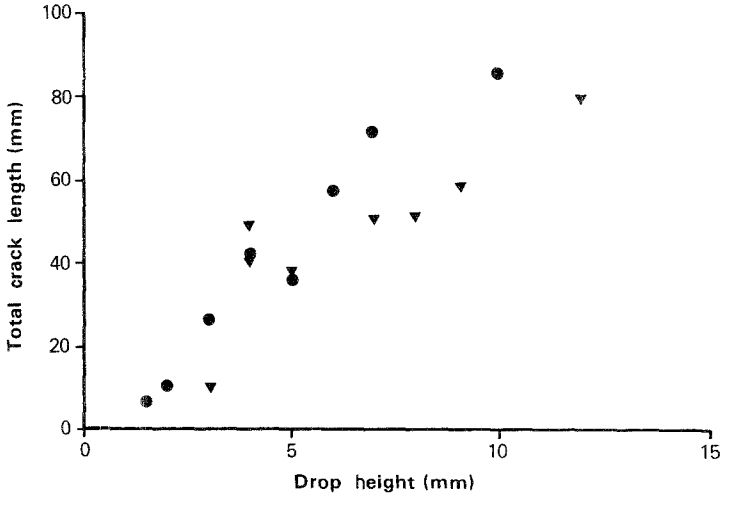

Figure 3 Cavity bias. Compound PA-1; (●) left-hand cavity, (▼) right-hand cavity. Specimens from the left-hand cavity crack more readily than those from the right hand one.

TABLE III The effect of impact velocity (Laboratory P)

Polymer Grade	Ratio of value at 3 m sec^{-1} to that at 5 m sec^{-1}				
	First peak			Total failure	
	Force	Deflection	Energy	Deflection	Energy
PA-1	1.02	1.02	1.19	0.91	0.97
PA-2	1.11	0.96	1.10	0.92	1.01
PA-3	1.15	0.99	1.20	0.93	1.06
PA-4	0.78	1.05	0.60	0.96	0.95
PA-5	0.64	1.11	0.51	0.91	0.91
Mean values (standard deviation)	0.94 (0.22)	1.03 (0.06)	0.92 (0.34)	0.93 (0.02)	0.98 (0.06)

Table III in the form of ratios relating the value of a specified quantity as measured at 3 m sec^{-1} to its value as measured at 5 m sec^{-1}. One cannot regard the 25 ratios as being all entirely independent but, for example, of the ten energy ratios (which are independent) five are less than unity and five are greater; they have a mean value of 0.95 and a standard deviation of 0.23. The only conclusions to be drawn from Table III are that the experimental scatter is high and any effects due to the change in impact velocity are either undetectable within that scatter or negligible.

The impact velocity was varied for only two of the grades in Laboratory Q. The results, which are presented directly rather than as ratios in Table IV, imply the same conclusion with respect to Feature A but the quantities related to the main peak and to total failure could be interpreted as indicating an increase in impact resistance with increasing impact velocity. There is evidence (see [1] and later in this paper) that in these experiments the apparent energy associated with total failure was greater than the true value because of an extraneous contribution from the broken segments as they resisted being forced into the support ring by the advancing impactor, and therefore the results in Table IV pertaining to total failure have to be discounted as evidence of a sensitivity to impact velocity. In contrast, the data relating to the main peak may be more reliable as evidence. A hint is to be found in the tabulated forces which show that the difference between Feature A and the main peak increases as the impact velocity increases, thereby producing some discrimination and also implying that the shape of the force–time response curves is affected by the velocity, as indeed is the case. In Fig. 4, the force–time curves for an impact velocity of 1 m sec^{-1} differ markedly from those for an impact velocity of 5 m sec^{-1}. At the lower velocity the force rises steadily, apart from extraneous vibrations to a simple well-defined peak, which is almost as high as the main peak or even constitutes the main peak, whereas at the higher velocity the force rises at a reduced rate after Feature A. Even if one disputes the real significance of that first feature, there remains the fact that the two response curves have different shapes, which clearly cannot be attributed to differences in the extraneous vibrations.

The statistically insignificant trend in the data from Laboratory P (Table III) is nevertheless consistent with the overall implications of the data from Laboratory Q and a few other results for one grade tested in a different configuration in Laboratory W show the same trend. In those tests, compound PA-4 moulded into edge-gated discs 100 mm in diameter and 3 mm thick were supported on a ring of internal radius 25 mm and impacted with a hemispherical striker tip 6.35 mm in diameter at velocities of 3, 4 and 5 m sec^{-1}. The derived values are again expressed as ratios, in Table V. As with the data from Laboratory P there is high experimental scatter but again the overall trend supports the tentative contention that the energy absorbed during impact failure and the impact strength increase with impact velocity. However, the important words are "trend" and "tentative" because the observed influence of impact velocity in the various sub-programmes was only slight over the range explored. Thus, any conclusions about the relative merits of the five materials are unlikely to be reversed or even modified by a modest change in the impact velocity, and for the purposes of this paper a comparison can be made between the five materials at whatever impact velocity is the most convenient. At the start of the programme, before the practical difficulties had been encountered and various issues resolved, there had been a loose agreement that data

TABLE IV The effect of impact velocity (Laboratory Q)*

Polymer Grade	Impact velocity (m sec^{-1})	Feature A (see Section 2)			Main Peak			Total failure	
		Force (N)	Deflection (mm)	Energy (J)	Force (N)	Deflection (mm)	Energy (J)	Deflection (mm)	Energy (J)
PA-3	1	504 (62)	1.9 (0.2)	0.41 (0.11)	790 (45)		1.6 (0.2)	9.0 (1.2)	4.0 (0.8)
	5	520 (47)	1.3 (0.1)	0.21 (0.03)	883 (63)	4.9 (0.3)	2.1 (0.5)	13.7 (2.8)	5.5 (0.7)
PA-5	1	444 (63)	1.8 (0.2)	0.35 (0.08)	484 (41)		0.5 (0.1)	6.6 (1.1)	1.8 (0.2)
	3	492 (11)	2.1 (0.1)	0.40 (0.03)	575 (30)		1.0 (0.4)	8.8 (0.3)	2.5 (0.1)
	5	460 (38)	1.6 (0.3)	0.28 (0.06)	592 (34)		1.3 (0.3)	10.4 (0.9)	2.7 (0.3)

*Figures in brackets are standard deviations.

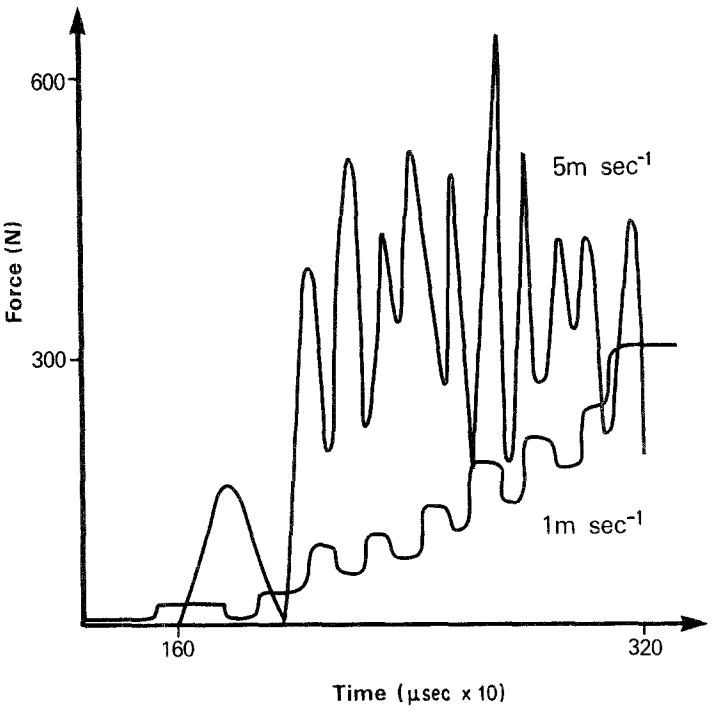

Figure 4 Response curves for two impact velocities. Nature of response varies with impact velocity.

for inter-laboratory comparisons might usefully be generated for an impact velocity of 5 m sec^{-1}, and it has transpired therefore that there are more data relating to that velocity than any other.

3.3. Comparative data on five grades

The data from Laboratory W are the best starting point if only because the associated software produces histograms showing the distribution of property values, superimposes histograms for other sub-sets and calculates the statistical significance of the difference between means. The mean values and standard deviations of the energy to the first peak and the total energy to failure obtained in that laboratory by tests at 5 m sec^{-1} on five matched pairs (i.e. left-hand and right-hand cavities) of specimens of each grade are given in Table VI. The statistical significance of the differences in the impact energies that are nominally attributable to the length of the fibres and to the two matrices (refer to Table I) are also shown. It is clear from Table VI that increased fibre length enhances the impact resistance; the force and the deformation are both increased and so also, of course, is the energy. The same picture emerges from the tests at 5 m sec^{-1} carried out in Laboratory P, from tests at 3 m sec^{-1} in the same laboratory and from tests at 1 m sec^{-1} on specimens from the right-hand cavity in Laboratory Q, though in the latter case it appears that the magnitude of the force, and the associated energy, at Feature A tends to decrease as fibre length increases. Those various results, with the exception of those relating to Feature A, are summarized in Table VII, in which the forces and energies are reduced to "enhancement ratios" which give the degree of improvement attributable to longer fibres. The table demonstrates very clearly that the longer fibres confer greater impact resistance; it also reinforces the picture presented in Part 1 [1] of poor quantitative agreement between the results emanating from the three collaborating laboratories. The contrary trend implied by Feature A gives enhancement factors less than unity when the same convention is observed, namely 0.73 for a weight fraction of 0.3 of glass fibres and 0.95 for a weight fraction of 0.5. The overall judgement that the longer fibres are beneficial disregards this particular indicator, but see further comments in Section 4.

Supplementary evidence is hardly necessary, but it is to be had from both the photographed impact tests and the low-energy-blow tests. A series of photographed impact events on any one sample enables the energy absorbed up to that point to be plotted against total crack length as seen in the photographed face (i.e. the tensioned face). The total crack length is measured with a digitizing slab which can accurately follow all routes that the crack follows. If the deformation of the specimen is relatively small, then the accuracy of this technique is adequate. However, once the crack opens and the deformation of the tension surface becomes larger then the measurement of total

TABLE V The effect of impact velocity (Laboratory W, compound PA-4)

Impact velocity (m sec^{-1})	Ratio of value to that at 5 m sec^{-1}				
	First peak			Total failure	
	Force	Deflection	Energy	Deflection	Energy
3	0.98	1.00	1.00	0.90	0.87
4	0.89	0.93	0.81	0.83	0.79

TABLE VI Comparison of materials (Laboratory W, impact velocity 5 m sec^{-1})*

Polymer Grade	First peak				Total failure		
	Force (N)	Displacement (mm)	Energy (J)	Significance of difference in energy†	Displacement (mm)	Energy (J)	Significance of difference in energy†
PA-1	666 (41)	2.5 (0.6)	0.8 (0.4)	HS†	10.4 (1.1)	4.1 (0.4)	HS
PA-2	878 (74)	4.1 (0.3)	1.9 (1.3)		16.8 (4.9)	7.2 (0.7)	
PA-3	709 (55)	4.5 (0.6)	1.8 (0.4)	HS†	14.5 (5.2)	5.5 (1.1)	HS
PA-4	697 (57)	2.7 (0.1)	0.7 (0.1)		11.4 (0.9)	3.7 (0.2)	
PA-5	591 (50)	2.7 (0.1)	0.6 (0.1)	HS	13.1 (1.6)	3.5 (0.3)	S

*Figures in brackets are standard deviations.
†S = significant, HS = highly significant.

crack length becomes an underestimate. Fig. 5 illustrates a set of data where the arrowed data point relates to an underestimated crack length. Fig. 6 illustrates a typical photographed tension surface, accompanied by a force–deflection curve.

It can be expected that the energy–crack length curve should not pass through the origin, because a finite strain energy would be necessary to deform a specimen prior to crack initiation. The magnitude of this energy could not be accurately measured from the limited number of photographed impact experiments, but is of the order of 0.1 J. The inability to monitor this energy has resulted in an imperfect analysis where curves are fitted to the data as straight lines which pass through the origin. Consequently, analysis of these plots in terms of determination of a notional fracture surface area (energy per unit crack length per unit specimen thickness) can only provide approximate values. The limited number of data also prevents a more detailed analysis. The fit of a straight line to the energy–crack length data is better for the mouldings with longer fibre lengths (PA-2 and PA-3) and least good for the mouldings with shorter fibre lengths (PA-1, PA-4, PA-5).

Setting aside, for the present, any doubts that there may be about the reliability of those data and making crude assumptions about the crack profile and about the microstructure of the fracture surfaces, notional "fracture surface energies" can be derived from both the photographed impact and the low-energy impact data. Surface energy values for specimens from the right-hand cavity are given in Table VIII. The superiority conferred by the longer fibres is clear despite the disparities between the two columns. The latter is not a cause for concern because the two sets of data are not strictly comparable (but see Section 4 for comments).

Turning now to the differences between compounds PA-4 and PA-5, which are based on nylon 6:6 and nylon 6 respectively, the relative impact resistances are shown, as ratios, in Table IX. Data relating to Feature A are again omitted, to ensure simplicity in the table

TABLE VII The enhancement of impact resistance attributable to fibre length

Laboratory	Impact velocity (m sec^{-1})	Weight fraction of fibre	Enhancement factors*		
			First peak force	Energy to first peak	Total failure energy
W	5	0.50	1.40	2.37	1.76
	5	0.30	1.02	2.57	1.49
P	5	0.50	1.38	1.40	1.48
	5	0.30	1.22	1.35	1.26
	3	0.50	1.29	1.30	1.54
	3	0.30	1.15	2.72	1.41
Q	1	0.50	1.14†	2.47	1.56
	1	0.30	1.07†	1.66	1.42

*Defined as (property value for long-fibre compound)/(property value for corresponding short-fibre compound).
†Data from Laboratory Q refer to main peak (i.e. maximum).

TABLE VIII Notional fracture surface energies from photographed impact and low-energy-blow experiments (specimens from right-hand cavity)

Polymer Grade	Fibre weight fraction	Fibre length	Notional fracture surface energy (kJ m^{-2})	
			Photographed impact (Laboratory W)	Low-energy-blow (Laboratory Q)
PA-1R	0.50	Short	10.4	16.5
PA-2R	0.50	Long	16.7	22.0
PA-3R	0.30	Long	11.8	–
PA-4R	0.30	Short	8.5	~11*
PA-5R	0.30	Short	8.1	~11*

*Insufficient data for precise quantification.

TABLE IX The relative impact resistance of PA-4 and PA-5

Laboratory	Impact velocity ($m\,sec^{-1}$)	Property ratio (value for compound PA-4)/(value for compound PA-5)		
		First peak force	Energy to first peak	Total failure energy
W	5	1.18	1.17	1.06
P	5	1.22	0.98	1.16
	3	1.16	1.14	1.22
Q	1	1.30*	1.56	1.30

*Main peak (i.e. maximum).

as before, but in this case they are in harmony with the mean peak data, rather than in conflict with it, and compound PA-4 has indisputably the greater impact resistance.

4. Discussion

The superior impact resistance of the compounds containing the longer fibres is so clearly demonstrated by the data that no discussion of that particular aspect of the results is necessary, except in relation to the contrary evidence embodied in Feature A. If that feature could be directly associated with fracture initiation one could then rationalize the results via the argument that at a given volume fraction of fibres there are more fibre ends, and hence more potential stress concentrators, in the compound with the shorter fibres, but the photographs published in Part 1 [1] failed to establish any close link between Feature A and the instant of crack initiation.* The low-energy-blow tests hinted at a reversed order of merit at short crack lengths but the apparatus is not sufficiently sensitive to resolve the issue beyond reasonable doubt at present. Apart from that, the straining rate decreases to zero during the course of the impact event in the low-energy-blow experiments, which may invalidate any comparisons that entail fine discrimination. The same fact may account for the numerical differences between the two sets of notional fracture surface energies in Table VIII. That said, these values are not grossly unreasonable, though there is a dearth of published information with which they can be compared, partly because injection moudings of fibre-reinforced polymers are layered structures with point-to-point variations in the orientation of the fibres and partly because of careless documentation in the past. Unpublished information available to the authors on a standard grade containing 0.33 weight fraction of short fibres tested in the form of "dry" notched Charpy bars, with a notch tip radius of 0.25 mm but axis unspecified, appear to have had an impact energy of about $7\,kJ\,m^{-2}$. Data published recently by Bailey and Bader [6] for a nylon 6, 6 reinforced by 0.25 weight fraction of short glass fibres indicate a notched Charpy energy of $5.85\,kJ\,m^{-2}$ (notch geometry unspecified, crack direction perpendicular to the main flow axis) and fracture surface energy from slow bend tests on the same specimen geometry of $8.57\,kJ\,m^{-2}$. This suggests that the values derived from the photographed impact experiments are approximately correct. Any rationalization of these results involves the different test geometries since the critical quantity is the energy density at the failure site and not the integrated energy. A subsidiary complication is that the fracture surfaces generated in these compounds are quite different from the surfaces created by the fracture of a glass; they are rough and fragmented to a depth of about 0.5 mm, so much so that it may be more profitable to think of the fracture event as entailing the disruption of a volume rather

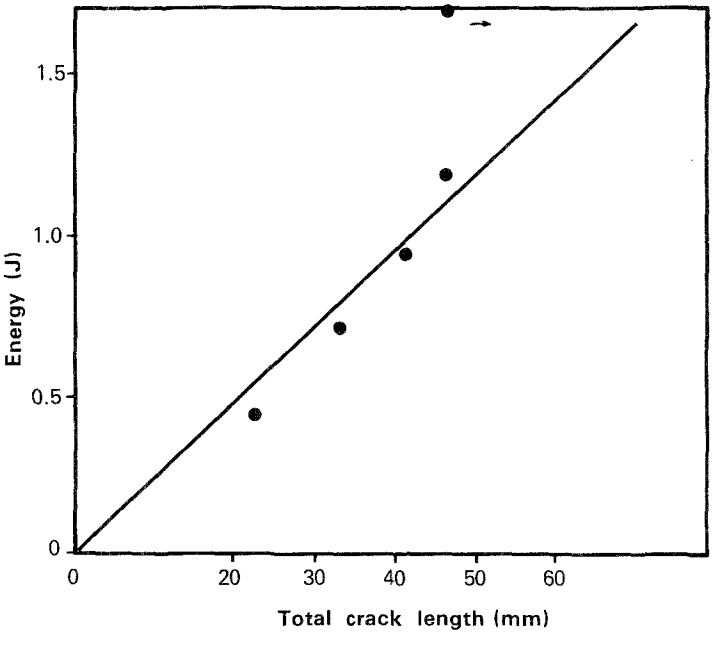

Figure 5 Notional fracture surface energy from photographed impact experiments, Compound PA-3R. G_c = slope/thickness = $11.8\,kJ\,m^{-2}$.

*New light has been shed on this issue by recent experiments that will be reported separately.

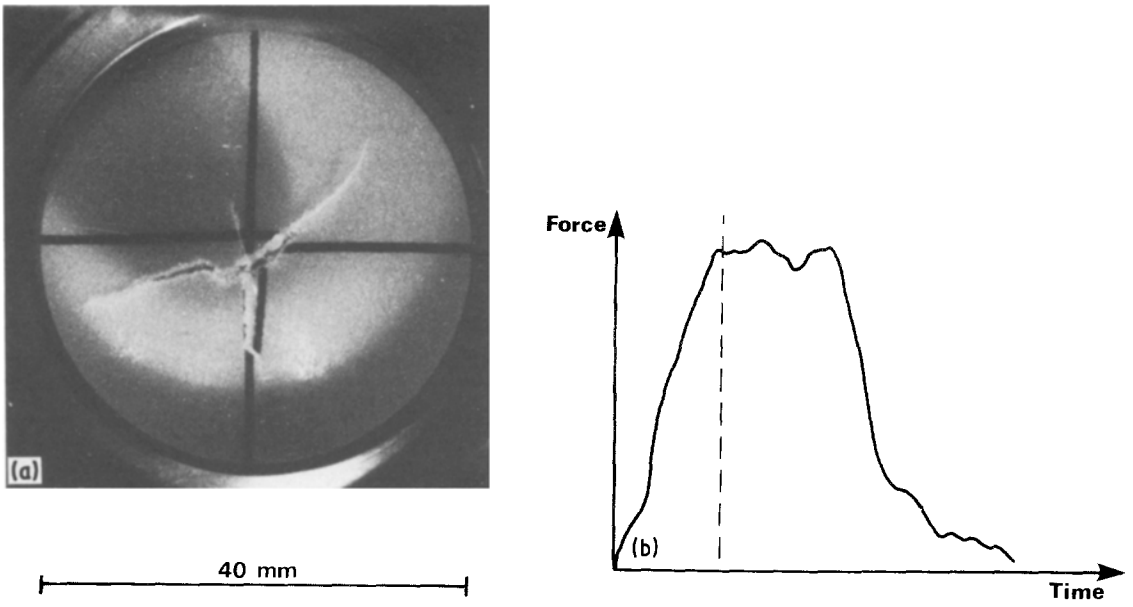

Figure 6 (a) Photographed impact, tension face during impact. Compound PA-3. (b) Event and response curve. The dashed line marks the instant of the flash.

than the creation of a surface. Be that as it may, if the energies to the first peak and the total energies from Table VI are combined separately with the notional fracture surface energies from the photographed impact experiments (Table VIII), the results can be converted into total crack lengths, and those calculated quantities are presented in Table X.

A detailed analysis of the values in Table X can only be pursued through the accommodation of several speculations. Nevertheless, a superficial analysis helps to examine some of the fundamental aspects of interpretation of the force–time signals that are monitored during impact experiments. The calculated notional crack area for initiation and propagation of a crack from the central stress field to the supports is given by

$$(A)_{CAL} = A_r nm$$

where n is the number of radial crack fronts, m is a "meandering factor" for a crack front and A_r is a radial crack area (for a 20 mm radius and specimen thickness of 2 mm, then $A_r = 40\,mm^2$). Values for n and m can only be guessed. For example, $n = 3$ to 4 seems likely and m can be assumed to be 1.5. Therefore the product nm might be in the range 4.5 to 6. Consequently, a maximum value for $(A)_{CAL}$ is $240\,mm^2$.

With reference to the calculated area factors in Table X, this clearly implies that the fracture process is more closely related to a notional first peak than to the apparent total energy absorption process.

In terms of future studies and procedures, then, a clear message emerges. The initiation and propagation events in impact are associated with the early parts of a force–deflection signal. In terms of any serious study of materials, whether associated with material comparisons or mechanistic characterization, there simply has to be better interpretation and understanding of the measurements in instrumented falling weight experiments.

TABLE X Crack growth in relation to response curves (Laboratory W)

Material code	Calculated area of crack that could be generated to first peak* (mm^2)	Calculated area of crack that could be generated by the total energy* (mm^2)
PA-1	160	780
PA-2	220	860
PA-3	300	940
PA-4	160	860
PA-5	140	860

*See Table VI.

Acknowledgements

Two of the authors (P.E.R. and S.T.) gratefully acknowledge the financial support of the Polymer Engineering Directorate.

References

1. A. E. JOHNSON, D. R. MOORE, R. S. PREDIGER, P. E. REED and S. TURNER, *J. Mater. Sci.* **21** (1986) 3153.
2. P. A. GUTTERIDGE, C. J. HOOLEY, D. R. MOORE, S. TURNER and M. J. WILLIAMS, *Kunststoffe, German Plastics* **72** (9) (1982) 10.
3. J. M. LUNT and J. B. SHORTALL, *Plast. Rubb. Processing* **4** (3) (1979) 108.
4. D. R. MOORE and R. S. PREDIGER, *J. Amer. Chem. Soc.* in press.
5. D. P. JONES, D. C. LEACH and D. R. MOORE, *Plas. Rubb. Processing Applic.* **6** (1) (1986) 67.
6. R. BAILEY and M. BADER, in Preprints of PRI Conference on Impact Testing and Performance of Polymeric Materials, Guildford, September 1985 (Plastics & Rubber Institute).

Received 20 June
and accepted 18 August 1986